

## Very-near-field plume study of a 1.35 kW SPT-100

**Sang-Wook Kim**

*Michigan Univ., Ann Arbor*

**John E. Foster**

*Michigan Univ., Ann Arbor*

**Alec D. Gallimore**

*Michigan Univ., Ann Arbor*

**AIAA, ASME, SAE, and ASEE, Joint Propulsion Conference and Exhibit, 32nd, Lake Buena Vista, FL, July 1-3, 1996**

Ion current density and electron number density profiles were measured in the very-nearfield plume of a 1.35 kW stationary plasma thruster (SPT-100). In order to take these measurements without significantly disturbing plasma flow while data were collected, a small Faraday probe and a single Langmuir probe were constructed and used with high-speed electronics for fast spatial sweeps. The data showed that there were distinct peaks in ion current density and electron number density related to the position of the thruster discharge chamber exit in the very-near-field plume. These peaks decreased and broadened as the axial position from the thruster exit increased. The Faraday probe data showed that a diverging annular ion beam came out of the discharge chamber. The inner boundary converged at or near 100 mm downstream of the exit plane. The Langmuir probe data gave insight to the competing effects between magnetic field confinement and diffusive processes. (Author)

## Very-Near-Field Plume Study of a 1.35 kW SPT-100

Sang-Wook Kim\*\*, John E. Foster\*\*, and Alec D. Gallimore\*  
Plasmadynamics and Electric Propulsion Laboratory  
Department of Aerospace Engineering  
The University of Michigan  
Ann Arbor, MI 48109-2118

### Abstract

Ion current density and electron number density profiles were measured in the very-near-field plume of a 1.35 kW stationary plasma thruster (SPT-100) loaned from Space Systems/Loral and Fakel Enterprises. In order to take these measurements without significantly disturbing plasma flow while data were collected, a small Faraday probe and a single Langmuir probe were constructed and used with high-speed electronics for fast spatial sweeps. The data showed that there were distinct peaks in ion current density and electron number density related to the position of the thruster discharge chamber exit in the very-near-field plume. These peaks decreased and broadened as the axial position from the thruster exit increased. The Faraday probe data showed that a diverging annular ion beam came out of the discharge chamber. The inner boundary converged at or near 100 mm downstream of the exit plane. The Langmuir probe data gave insight to the competing effects between magnetic field confinement and diffusive processes.

### Introduction

The stationary plasma thruster (SPT) developed in the former Soviet Union has been under intensive investigation in the U.S. for the past several years. High efficiency and high specific impulse at low power levels make this device attractive for north-south station-keeping[1]. In addition, these features are particularly appealing for the New Millennium spacecraft series whose main emphasis is on smaller, lighter, and less expensive systems. The

obvious commercial interests in near-earth space missions have led the overwhelming bulk of SPT development activities to focus on performance, lifetime, and integration issues in an effort to fully flight-qualify the thrusters. As a result, the baseline operating conditions of SPTs are now well established. The next step is to broaden the operating parameters of the SPTs such as operation on Krypton or Oxygen[2]. However, more understanding of SPT thruster physics is necessary to achieve this end.

To this end, the very-near-field plume of the SPT-100 was investigated. Radial profiles of ion current density and electron number density were obtained at various axial positions. These maps provide insight to the operation of these devices. These maps will also support code development activities[3].

### Experimental Apparatus

The stationary plasma thruster studied in this work is the Fakel SPT-100[4,5]. The discharge chamber of this device consists of an annular anode with inner and outer diameters of 56 mm and 100 mm, respectively. An external, side-mounted hollow cathode located at 270 degrees serves as the electron source. The power processing unit, which was powered by a single 55 V-55 A power supply, regulated power to the discharge, the cathode heater, the electromagnets, and thermothrottle. The operating point that was investigated with this thruster was 300 V and 4.5 A with a total xenon flow rate of 5.5 mg/s.

Experiments were conducted in a 9-m-long by 6-m-diameter stainless-steel vacuum chamber. This chamber is evacuated by six 81 cm oil diffusion pumps backed by two blowers

---

\* Assistant Professor, Member AIAA

\*\*Graduate Assistants, Member AIAA

and four mechanical pumps. In addition, a Polycold water cryopump located above two of the oil diffusion pumps enhanced the overall water pumping speed. The total xenon pumping speed for this facility was in excess of 25,000 l/s at  $10^{-5}$  Torr. Chamber pressure was measured with two hot cathode ion gauges. During thruster operation, the background pressure was  $3 \times 10^{-5}$  Torr.

The primary diagnostics used in this very-near-field study included a Faraday probe and a single Langmuir probe. The Faraday probe consisted of a 2.4 mm diameter tungsten rod that was surrounded by an alumina sleeve so that only the end surface was exposed to the plasma. A guard ring was not used because the thickness of the protective alumina sleeve which would otherwise separate the ring from the actual probe was much larger than a Debye length. The cylindrical Langmuir probe used in this work consisted of a 0.127 mm diameter, 0.88 mm long tungsten wire collection surface which was separated from the remaining wire via a Pyrex casing. A half-and-half mixture of hydrofluoric and nitric acids was used to trim the tip of the tungsten wire. This casing was further protected by an alumina sleeve that fit over the casing's outer surface.

In order to acquire the axial and radial near-field profiles, the probes were mounted to a custom-made probe positioning system developed by NEAT (New England Affiliated Technologies). The radial table provides roughly 188 cm of travel while the axial table provided up to 91 cm of travel. The radial translation speeds, which are in excess of 60 cm/s, allows for quick sweeps in and out of the plume thus avoiding excessive heating of the probes. The translation stages are controlled by a Macintosh-based control system coordinated by a National Instrument's LabVIEW platform.

Plasma data from both probes were obtained using the circuit illustrated in Figure 1. The collection electrode is biased relative to tank ground using a Kepco bipolar power supply. The current signal is measured via an operational amplifier which sends the voltage signal which develops across the 10.02 k $\Omega$  resistor to a Tektronics TDS 540 digital oscilloscope. The probe voltage is sent directly to the oscilloscope. The current-voltage characteristic stored in the oscilloscope is then exported for analysis to a computer using a National Instruments GPIB interface. In the case of the Langmuir probe, the bipolar power supply's voltage was ramped in order to obtain the current voltage characteristic. In the case of the Faraday probe, the collector was maintained at a bias voltage of -47 V with

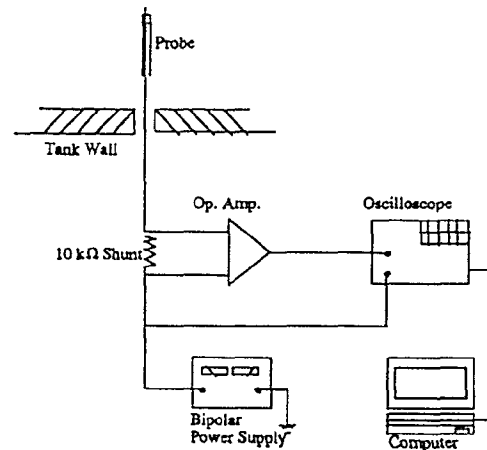


Figure 1: Probe Circuit

respect to ground to repel electrons and thus collect primarily the ion flux.

### Results and discussion

For this investigations, the SPT-100 was operated at a nominal discharge of 300 V and 4.5 A. Typical cathode to ground voltage was -20 Volts. The SPT-100 used xenon propellant at a flow rate of 5.5 mg/s total with 0.28 mg/s of this going through the hollow cathode. The SPT-100 was stable over the measurement period. Prior to taking measurements, the thruster was allowed to run approximately 30 minutes to reach thermal equilibrium.

Measurements of ion current density and electron number density using the miniature probes described in the previous section are presented. All radial profile measurements were taken in steps of 5.08 mm (0.2 in.) from the center line of the thruster (0 mm position) to 200 mm outward opposite to the side where the cathode is located. The axial position was varied from 10 mm to 200 mm downstream of the exit plane.

To collect data this close to the exit plane, the probes were quickly moved to the collection site, kept there long enough to collect data (~0.5 sec.), and rapidly moved out of the plasma flow to allow for probe cooling. This approach also served as an effective means of cleaning the probes.

### Ion current density

Figure 2 shows the radial distributions of ion current density measured at different axial positions. There is an uncertainty of  $\pm 10\%$  in these measurements. At 10 mm downstream of

the exit plane the ion current density has a very sharp and large peak in front of the thruster discharge chamber. This indicates that the ions are coming out of the thruster channel as a narrow beam, perhaps narrower than the width of the chamber. Farther downstream, the peak in front of the chamber decreases in magnitude and broadens. This implies that the ions are diverging from the exit of the thruster channel.

At a larger axial location, the ion current density at 0 mm radial position (on centerline) increases and forms a peak. These peaks are attributed to the fact that the diverging annular ion beam overlaps at the centerline of the thruster. The ion current density at the center increases up to the 100 mm axial position, and then begins to decrease at larger axial positions. This implies that the inner boundary of the annular ion beam converges on the centerline at or near 100 mm from the exit plane and defocuses at larger axial positions. In addition to the overlapping, another possible mechanism for the formation of these peaks is back scattering of ions off the background particles. Downstream of the focal point, the overlapping annular beam forms one broad plume. The flat ion density profile in front of the discharge chamber at the 100 mm downstream location in Figure 2 is another indication that this distance is where a transition is occurring. The ion densities at the center were normalized to a distance of 1 m from the thruster using a  $1/r^2$  dependence and were compared to previous studies[6]. The ion current density at 200 mm from the thruster was in good agreement with previous investigations. The ion current density at an axial location of 100 mm was, however, much higher than the calculated normalized value.

Total ion current at each axial location, calculated by integrating the ion current density plot, is tabulated below.

Table 1: Total Ion Current

axial position (mm)	total ion current (A)
10	3.97
25	4.92
50	4.95
100	4.51
200	3.86

The reason for the variation in total ion current along the thruster axis is not known at this time.

The probe angle was not varied. When the plasma flow is not perpendicular to the Faraday probe collection surface, the effective collection area is smaller, and thus the actual ion current density will be higher than what is measured. This error becomes larger as the probe

moves away radially. However, this effect was thought to be small at various axial positions directly beyond the thruster.

### Electron Number Densities

Because the probe radius is approximately seven times larger than the Debye length, and because the electron gyro-radius is several times larger than the probe radius, the standard collisionless thin sheath Bohm ion saturation current model was used to interpret Langmuir probe data.

Figure 3 shows the radial distributions of electron number density measured at different axial positions. There is an uncertainty of  $\pm 50\%$  in these measurements. There is a large sharp peak in front of the discharge chamber at 10 mm from the exit plane. This high electron number density can be attributed to three different sources of electrons: 1) electrons from cathode, 2) ionization processes, and 3) the secondary electrons produced by the high energy ions hitting the thruster chamber wall. This peak still exists at 100 mm downstream of the exit plane but disappears at 200 mm downstream. This finding further supports the conclusion drawn in the discussion of ion current density that the diverging annular ion beam overlaps on center line at or near 100 mm downstream of the thruster exit, forming one broad plume at farther axial locations.

There are also peaks on centerline. Those peaks at smaller axial positions on centerline are attributed to electrons confined by the magnetic field cusp formed by the thruster magnetic coils. Those peaks at larger axial positions on centerline are due to electrons attracted to the corresponding high ion density at those locations. The difference in size of these peaks at different axial positions is small compared to that of the ion current density profiles. Also, the center peaks of the electron number density are sharper than those of the ion current density. These show that the magnetic confinement of electrons is very strong.

The peak in front of the thruster discharge chamber becomes flatter as the axial position increases. This can be ascribed to the competition between the magnetic confinement effect, which dominates at axial distances close to the exit plane, and diffusive processes, which dominates farther downstream. One puzzling feature of the electron number density profiles in Figure 3 is that the electron number density at 200 mm axial position is higher than at intermediate axial positions. It may be attributed

to the re-distribution of electrons from the center of the plume.

The electron number density at large radial positions are larger than expected since the electron number density should decrease rapidly as a function of increasing radial position[7]. The error due to a misaligned probe cannot only affect the absolute values of the measured electron number density but the relative profiles as well. However, the error in ignoring flow perpendicular to the probe is small at various axial locations directly downstream of the thruster. It is well documented that supersonic ion flow, perpendicular to a cylindrical probe, increases the ion current significantly[8,9]. Since the ion saturation current was used to calculate the electron number density, the actual electron number density at those large radial positions would be much smaller than the measured electron number density, therefore explaining the unusually large density measured at large radial positions in this study.

Figure 4 shows the radial profiles of electron temperature measured at different axial locations. The collisionless thin sheath Bohm ion saturation current model predicts that there is an uncertainty of  $\pm 5\%$  in these measurements. At very close axial positions (10 mm and 25 mm), the electron current approached saturation very slowly, and thus, there was no clear saturation "knee" in the  $\ln(I_{\text{probe}} + I_{\text{ion}})$ -versus- $V_{\text{probe}}$  plots. Therefore, the slopes of those curves were taken at the probe voltages near the floating potentials. The data are consistent with an earlier study which measured electron temperature at the discharge chamber exit of a hall-current accelerator with an extended acceleration zone to be 12 eV with large spatial gradient[10]. However, this result did not agree with the emission spectra data taken in this study. This discrepancy will be discussed later.

#### The Equilibrium State at the Exit Plane

Xe II emission spectra were acquired along a chord extending across the cross section of the exit plane to determine the equilibrium state of the plasma near the source. By plotting  $\ln [ I_{k_i} \cdot \lambda_{k_i} / g_k \cdot A_{k_i} ]$  versus  $E_k / k_B$ , a Boltzmann excitation temperature was obtained, where  $E_k$  is the energy of the excited state,  $I_{k_i}$  is intensity of the transition,  $\lambda_{k_i}$  is the wavelength of the transition,  $A_{k_i}$  is the transition probability, and  $g_k$  is the degeneracy of the upper state[11]. At equilibrium, Figure 5 should be a straight line. Scatter in the Boltzmann plot obtained from the measured spectra suggests that the atomic energy

level populations are not completely in Local Thermal Equilibrium with the electrons. This is due in part to the low electron number density which is insufficient to collisionally dominate excitation and de-excitation processes. In any event, assuming that Partial Local Thermal Equilibrium exists, then one can approximate the electron temperature by using the excitation temperature. The Boltzmann plot's slope suggests an electron temperature of 2.7 eV. This result is consistent with an earlier study[12]. However, this temperature is smaller than that measured 1.0 cm downstream of the exit plane using a Langmuir probe by roughly a factor three. The discrepancy in temperature measurements is believed to be associated with magnetic field effects which tend to inflate the calculated temperature by reducing the slope of the Langmuir I-V characteristic in the electron retarding region. This then would explain why the Langmuir probe measured electron temperature near the exit plane is so large (~8 eV) and why the electron temperature decreases with increasing axial position. In this case, at larger axial positions the magnetic field effects are reduced due to a weaker field at those locations.

#### Conclusions

Radial profiles of ion current density and electron number density were measured at various axial positions in the very-near-field plume of a 1.35 kW SPT-100 operating at nominal condition of 300 V and 4.5 A at a total flow rate of 5.5 mg/s using xenon as the propellant.

The radial ion current density profiles exhibited a distinct peak structure. A sharp high peak in front of the discharge chamber at 10 mm downstream of the exit plane indicates that the ions were coming out of the chamber as a narrow beam. These measured peaks were observed to decrease in magnitude and broaden spatially in the radial direction with increasing axial position relative to the thruster exit plane.

The radial electron number density profiles also exhibited a distinct peak structure. A large sharp peak at 10 mm from the discharge chamber exit were attributed to electrons from the cathode, ionization processes, and the secondary electrons produced by high energy ions hitting the discharge chamber wall. The measured peaks downstream of the discharge chamber were observed to broaden into virtually a flat profile as the axial position increases. This behavior may be attributed to the competing effects of magnetic confinement and diffusive processes.

Large electron temperature values obtained from Langmuir probe data suggests that the magnetic field in the very near-field may be severely affecting the Langmuir probe current-voltage characteristic. Future studies will be made to investigate this effect.

#### Acknowledgments

One of the authors (S-W Kim) would like to thank all of his fellow students at the Plasmadynamics and Electric Propulsion Laboratory, especially J. Haas and G. Williams. S-W Kim also thanks Jongchun Ahn for providing his lab for the probe construction. We wish to thank Space Systems/Loral for the loan of the SPT-100 and the PPU.

#### Bibliography

1. Brophy, J.R., Barnett, J.W., Sankovic, J.M., and Barnhart, D.A., "Performance of the Stationary Plasma Thruster: SPT-100," AIAA-92-3155, July 1992.
2. Marreses, C., Gallimore, A.D., et.al., "An Investigation of Stationary Plasma Thruster Performance with Krypton Propellant," AIAA-95-2932, July 1995.
3. Oh, D. and Hastings, D., "Axisymmetric PIC-DSMC Simulations of SPT Plumes," IEPC-95-160, September 1995.
4. Garner, C.E., Brophy, J.R., Polk, J.E., and Pless, L.C., "A 5,730-Hr Cyclic Endurance Test of The SPT-100," AIAA-95-2667, July 1995.
5. Day, M., Maslennikov, N., Randolph, T., and Rogers, W., "SPT-100 Subsystem Qualification Status," AIAA-95-2666, July 1995.
6. Manzella, D.H. and Sankovic, J.M., "Hall Thruster Ion Beam Characterization," AIAA-95-2927, July 1995.
7. Ohler, S., Gilchrist, B., and Gallimore, A.D., "Microwave Plume Measurements of an SPT-100 using Xenon and a Laboratory Model SPT using Krypton," AIAA-95-2931, July 1995.
8. Sonin, A.A., "Free Molecular Langmuir Probe and its use in Flowfield Studies," AIAA J., Vol. 4, No. 9, 1966, pp. 1588-1596.
9. Godard, R. and Laframboise, J.G., "Total Current to Cylindrical Collectors in Collisionless Plasma Flow," Planet. Space Sci., Col.31, No. 3, 1083, pp. 275-283.
10. Bishaev, A.M. and Kim, V., "Local plasma properties in a Hall-current accelerator with an extended acceleration zone," Soviet Physics-Technical Physics, Vol. 23, 1978. pp. 1055-1057.
11. Griem, H.R., Plasma Spectroscopy, McGraw-Hill, New York, 1964.
12. Manzella, D.H., "Stationary Plasma Thruster Plume Emissions," IEPC-93-079, September 1993.



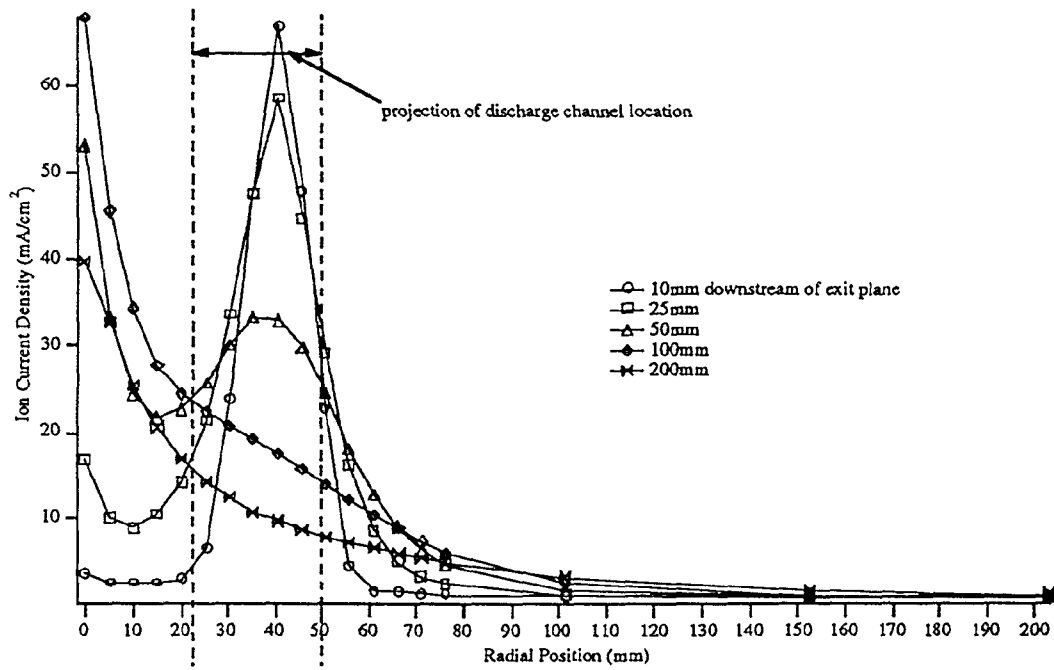


Figure 2: Radial Ion Current Density Profiles at Different Axial Locations

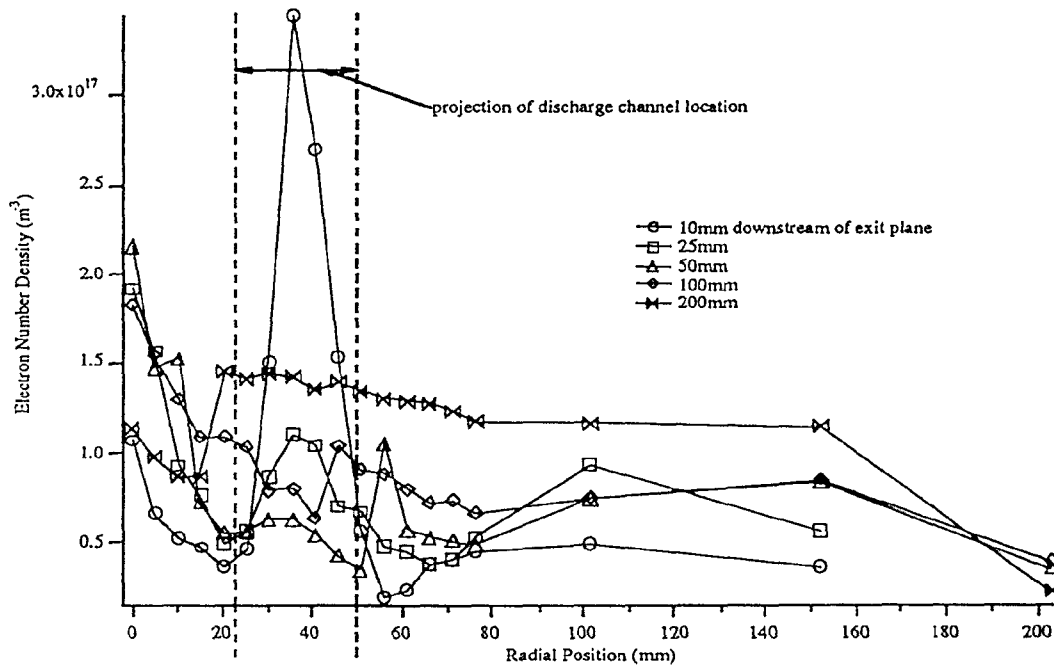


Figure 3: Radial Electron Number Density Profiles at Different Axial Locations

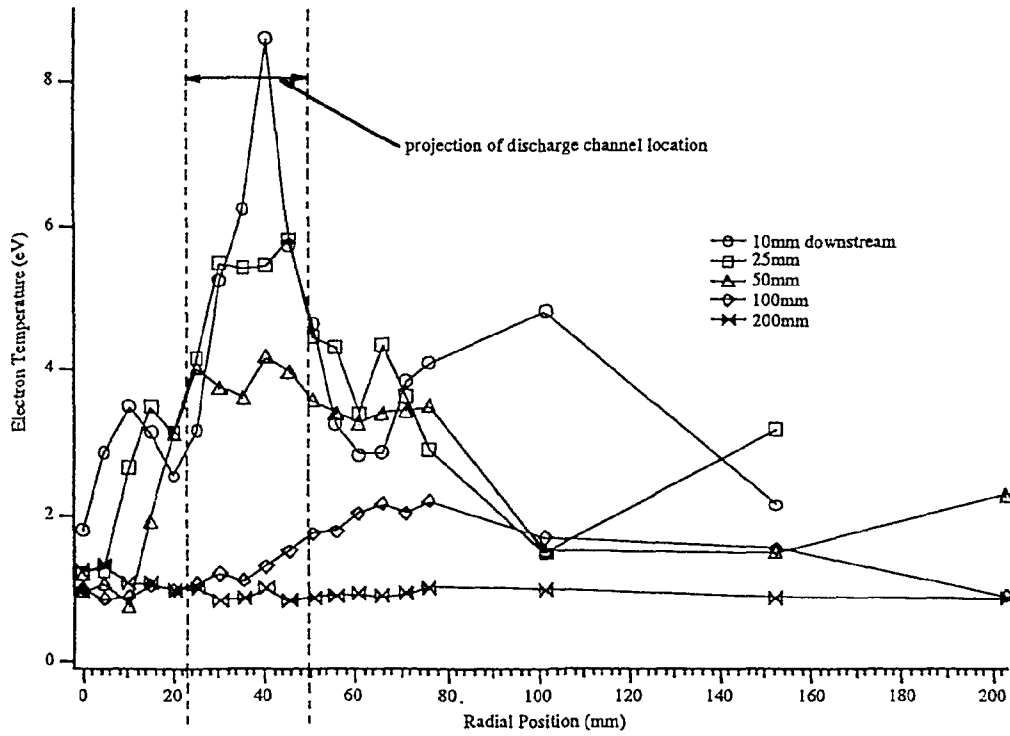


Figure 4: Radial Electron Temperature Profiles at Different Axial Locations

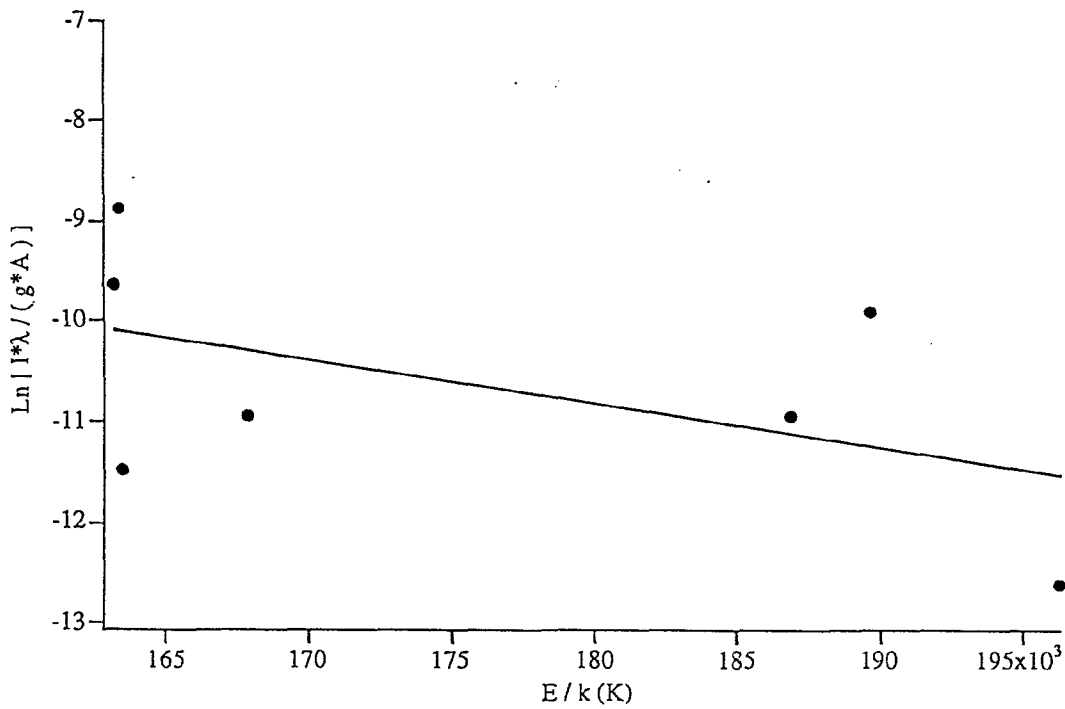


Figure 5: Boltzmann Plot for Xe II